NOTES AND CORRESPONDENCE

Extension of a Conservative Cascade Scheme on the Sphere to Large Courant Numbers

RAMACHANDRAN D. NAIR

Scientific Computing Division, National Center for Atmospheric Research,* Boulder, Colorado

ABSTRACT

The conservative cascade scheme (CCS) combines a one-dimensional mass-conserving finite-volume method with an efficient semi-Lagrangian scheme over the sphere. Major limitations of this scheme are a breakdown in the polar region due to the coordinate singularity and a restriction to polar meridional Courant number $C_\theta \leq$ 1. The proposed scheme is an extension of the CCS over the sphere for $C_\theta > 1$. This is achieved by isolating a region near the pole where the CCS fails and applying a two-dimensional remapping based on the cell-integrated semi-Lagrangian (CISL) scheme. The interface between these two schemes is the singular polar region where the total mass is computed and redistributed in a conservative manner. The resulting scheme is applicable to large polar Courant number and is tested using solid-body rotation and a deformational flow.

1. Introduction

Finite-volume-based semi-Lagrangian (SL) transport schemes are gaining importance in meteorological modeling (see, e.g., Lin and Rood 1996; Rasch 1998; Nair and Machenhauer 2002; Nair et al. 2002; Zerroukat et al. 2002). The main advantage of such "cell based" schemes is that they are formally conservative and stable for large time steps, which are desirable properties for global climate modeling. However, in spherical geometry with an orthogonal longitude–latitude (λ, θ) grid system, these schemes require special treatment. Polar singularities restrict the time step in such a way that the polar meridional Courant number $C_\theta \leq 1$; that is, the Lagrangian pole should be within the first latitude circle (see Lin and Rood 1996; Nair et al. 2002, 2003). Recently, Nair and Machenhauer (2002) have extented the cell-integrated semi-Lagrangian (CISL) scheme of Machenhauer and Olk (1996) in spherical geometry for $C_\theta < 2$. The scheme developed by Nair and Machenhauer (2002, hereafter referred to as NM02) employs a fully two-dimensional (2D) remapping scheme that requires storage of *accumulated coefficients* along the latitude circles. Recently, Nair et al. (2002, hereafter re-

ferred to as NSS02) have developed a "conservative cascade scheme" (CCS) over the sphere based on a cascade interpolation procedure (Purser and Leslie 1991; Nair et al. 1999). The CCS combines a conservative finite-volume method and a computationally efficient SL scheme based on a dimensional splitting cascade interpolation method.

In NSS02, the CCS is free from zonal Courant number C_λ restriction and is shown to be more efficient and less memory intensive than the CISL scheme while maintaining accuracy comparable to the CISL scheme (NM02). However, a major limitation of the CCS for global applications is the polar meridional Courant number restriction, $C_\theta < 1$ (NSS02). In this paper I present a procedure to overcome the meridional Courant number restriction of the CCS by combining the CCS with the CISL scheme in polar regions. In section 2, I briefly outline the CCS and CISL remappings and describe the extension procedure. In section 3, numerical results are presented, followed by concluding remarks in section 4.

2. Conservative SL schemes

To briefly describe the finite-volume-based conservative SL transport scheme as presented in NM02 and NSS02, consider the integral form of the mass-continuity equation in the absence of sources or sinks:

$$\frac{d}{dt} \int_{V(t)} \rho \, dV = 0, \qquad (1)$$

where d/dt is the total (Lagrangian) derivative, ρ is the density of the fluid, $V(t)$ is an arbitrary reference volume

Corresponding author address: Dr. Ramachandran D. Nair, Scientific Computing Division, National Center for Atmospheric Research, 1850 Table Mesa Drive, Boulder, CO 80305.
E-mail: rnair@ucar.edu

(moving with the fluid), and dV is the volume element. The quantity $\int_{V(t)} \rho \, dV$ in (1) may be interpreted as the mass of the fluid in the volume $V(t)$ and is constant along the flow trajectory. Integrating (1) along a trajectory, over a time step Δt, yields the two-time-level conservative SL scheme:

$$\overline{\rho}^{n+1} V^{n+1} = \overline{\rho}^n V^n, \tag{2}$$

where the superscripts n and $n + 1$, respectively, indicate departure and arrival time levels, and $\overline{\rho}$ is the cell- (volume) averaged density defined by

$$\overline{\rho} = \frac{1}{V} \int_V \rho \, dV.$$

For backward trajectory conservative SL methods, a departure cell is defined to be a Lagrangian (upstream) cell and the corresponding arrival cell is a regular Eulerian cell. Now, (2) predicts cell-averaged density $(\overline{\rho}^{n+1})$ at a new (future) time level if the mass $(\overline{\rho}^n V^n)$ in the Lagrangian cell is known. Thus, accurate computation of the mass enclosed in the Lagrangian cell is of fundamental importance and is accomplished by a remapping process.

a. CCS and CISL remapping

Global conservative schemes in NM02 and NSS02 exploit the transformation from a (λ, θ) spherical domain to a Cartesian plane by introducing an independent variable $\mu = \sin\theta$ such that $\mu \in [-1, 1]$ and $\lambda \in [0, 2\pi)$. In the (λ, μ) plane, Lagrangian cells are assumed to be quadrilaterals and the corresponding Eulerian cells are rectangles (see NSS02 for details). For the computational procedure, the Lagrangian cells are further approximated as polygons with sides parallel to either the λ- or μ-coordinate axis.

A major difference between the 2D CCS and CISL schemes is that the CCS sequentially applies one-dimensional (1D) remapping along the μ and λ directions, whereas the CISL scheme uses a fully 2D remapping strategy (NM02). The density distribution functions for the CCS and the CISL scheme are quite different and consistent with their respective remapping methods. The CCS uses cell averages to construct a unique piecewise parabolic polynomial (Colella and Woodward 1984) for each dependent variable within a cell. The density distribution for the CCS in the λ or μ direction can be generalized as follows:

$$\rho(\xi) = \overline{\rho} + h_1 \xi + h_2 \left(\frac{1}{12} - \xi^2 \right), \tag{3}$$

where $\overline{\rho}$ is the cell-averaged density, $\xi \in [-1/2, 1/2]$ is a normalized local variable, and h_1 and h_2 are coefficients in the μ or λ direction, depending on the direction of remapping.

However, the CISL scheme employs a quasi-biparabolic function for the density distribution, defined by

$$\rho(x, y) = \overline{\rho} + ax + b\left(\frac{1}{12} - x^2 \right) + cy$$
$$+ d\left(\frac{1}{12} - y^2 \right), \tag{4}$$

where $x, y \in [-1/2, 1/2]$ are the normalized local variables; a, b are the coefficients in the λ or x direction; and c, d are the coefficients in the μ or y direction, respectively (see NM02 for details).

In order to illustrate the extension process, we focus on the north polar region of the sphere. It is straightforward to extend the algorithm to the south polar region.

b. Extension of the CCS for large C_θ

The cascade interpolation procedure developed by Nair et al. (1999), on the sphere for nonconservative SL schemes, is free from Courant number limitations. In this algorithm, data is transferred from Eulerian points to Lagrangian points through a well-defined intermediate grid system by means of two 1D interpolations. However, the conservative version of cascade interpolation (NSS02) employs Lagrangian cells rather than Lagrangian points, thus imposing additional constraints and making it less flexible. For the CCS, mass from Eulerian cells is transferred to Lagrangian cells through an intermediate cell system. In NSS02, intermediate cells are defined by the intersection of Lagrangian latitudes and Eulerian longitudes (see Fig. 1 of NSS02). The area (length) of the cells (Eulerian, intermediate, or Lagrangian) involved in the cascade cycle play an important role in both local and global mass conservation.

For stability, the Lagrangian cells must be well defined. In other words, the cell walls should not intersect within a single time step (Lin and Rood 1996; NM02). In the polar region, (λ, μ) coordinates induce severe cell deformation. Even with a small meridional Courant number C_θ, Lagrangian cells in these regions are deformed. In particular, the Lagrangian cell containing the Eulerian pole point is not well defined (NM02). Two schematic figures are used to illustrate this situation.

Figure 1a shows the north polar region in spherical (λ, θ) coordinates projected onto a polar tangent plane. The dashed circles and straight lines represent Eulerian latitudes and longitudes, respectively. The corresponding Lagrangian latitudes and longitudes are depicted as ellipses and solid smooth curves, respectively. The Eulerian pole is shown as an open square and the corresponding Lagrangian pole is shown as a solid square. Solid circles in both Figs. 1a and 1b represent Lagrangian points. Figure 1b is the schematic illustration of Fig. 1a in the (λ, μ) plane, where Eulerian latitudes and longitudes are shown as dashed straight lines. In Fig. 1b, the line $\mu = 1$ corresponds to the Eulerian pole point, and the Lagrangian latitudes are denoted by solid
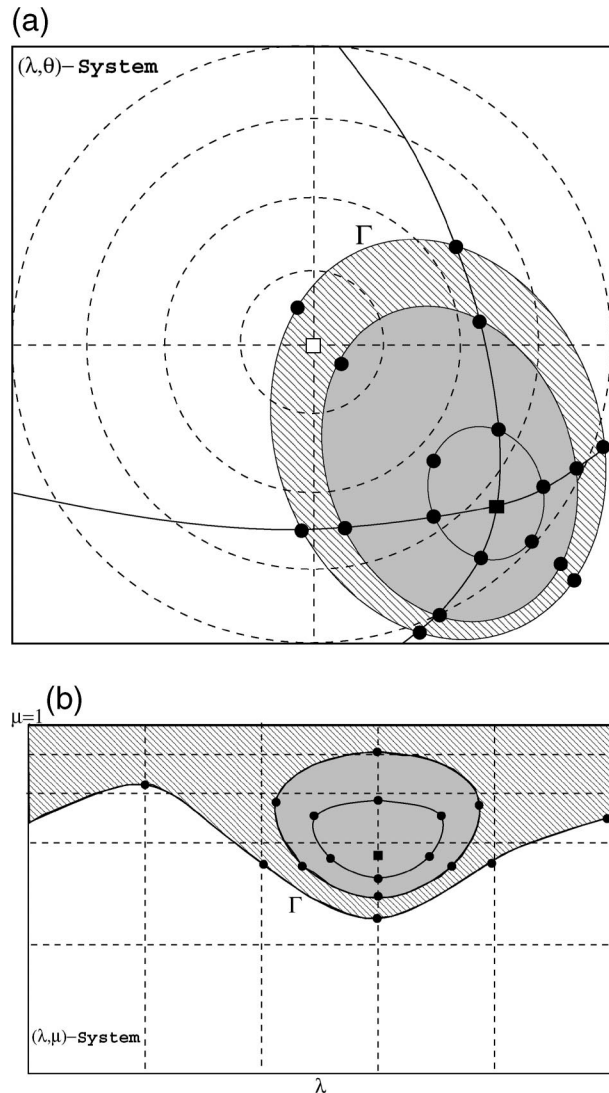
(a)

(b)

FIG. 1. (a) Schematic of Eulerian and Lagrangian cells over the polar regions in (λ, θ) coordinates, as projected onto a polar tangent plane. The dashed lines show the Eulerian latitudes and longitudes. Corresponding Lagrangian latitudes and longitudes are denoted by ellipses and solid curves, respectively. The Lagrangian pole point is marked by a solid square, the corresponding Eulerian pole is marked by an open square, and solid circles represent the Lagrangian points. (b) Same as (a), but the Eulerian and Lagrangian lines (points) are mapped onto the (λ, μ) plane. The line $\mu = 1$ is the pole line corresponding to the Eulerian pole point in (a). The solid curve Γ defines the north boundary for the CCS. The polar singular region (see text) is depicted as the hatched region. The CISL scheme is applied in the shaded region bounded by closed curves.

curves. Lagrangian cells in the CCS and the CISL scheme are constructed by joining the Lagrangian points as the corner points of a rectangle. However, this approach is impractical or too crude for certain polar Lagrangian cells in the (λ, μ) plane. This is schematically illustrated in Fig. 1b, where the hatched area represents a region in which Lagrangian points close to the Eulerian pole line $\mu = 1$ fail to form a Lagrangian cell.

Moreover, in the (λ, μ) plane, the cell that includes the Eulerian pole (singular point) is located in this region and it is not well defined. In NM02, such a region is referred to as the "polar singular belt (region)"—this terminology is used henceforth. The usual remapping process of CISL or CSS fails in such regions.

A cost-effective way to avoid this problem is described in NM02 and NSS02. This involves introducing additional points along the polar Lagrangian cell walls (in the μ direction) and redistributing mass in an array of cells located in the polar singular belt (see NM02 for details). The CISL approach in NM02 accurately simulated cross-polar advection for $C_\theta < 2$, and we extend this idea for the CCS when $C_\theta > 1$. Here, we treat the polar singular belt as the interface zone when combining the CCS and the CISL scheme. The resulting scheme is referred to as the extended CCS.

c. Computational procedure

When the meridional Courant number is large ($C_\theta \gg 1$), it is possible that not all the Lagrangian latitudes (around the Lagrangian pole) intersect with Eulerian longitudes (see Fig. 1a). This may adversely affect the generation of intermediate cells (NSS02) and may cause a breakdown of the conservative cascade process in polar regions. In order to proceed with cascade remapping, we isolate a region over the pole where intermediate cell generation is not obvious. In Figs. 1a and 1b such a region is shown as a closed region bounded by the curve Γ. The total mass (M_{CCS}) enclosed by Γ is determined from the first phase of remapping in the μ direction. The CISL scheme with 2D remapping is then used to compute the total mass (M_{CISL}) in the shaded region (Fig. 1b), within the region bounded by Γ. Note that the CISL scheme accurately estimates the mass enclosed in individual Lagrangian cells in the closed region (NM02). The total mass enclosed (M_{SB}) in the polar singular belt (hatched region in Fig. 1b) is simply the difference in masses, that is, $M_{SB} = M_{CCS} - M_{CISL}$. The computed total mass in the polar singular belt is then redistributed to the constituent cells by an efficient redistribution scheme suggested by NM02. This redistribution scheme is locally approximate but constrained in such a way that the total mass in the singular belt is conserved.

The location of the Lagrangian latitude that defines the northernmost boundary (the curve Γ in Figs. 1a,b) of the cascade process can be easily identified. It is the first Lagrangian latitude (in Fig. 1a, from the Lagrangian pole), that inscribes the Eulerian pole. In addition, the next Lagrangian latitude, within the region bounded by Γ, serves as the exterior boundary of a region where the CISL scheme is applied. Consequently, the polar singular belt acts as an interface between the regions where the CCS and the CISL scheme are applied. When $C_\theta \leq 1$, the region bounded by Γ is just the polar sin-
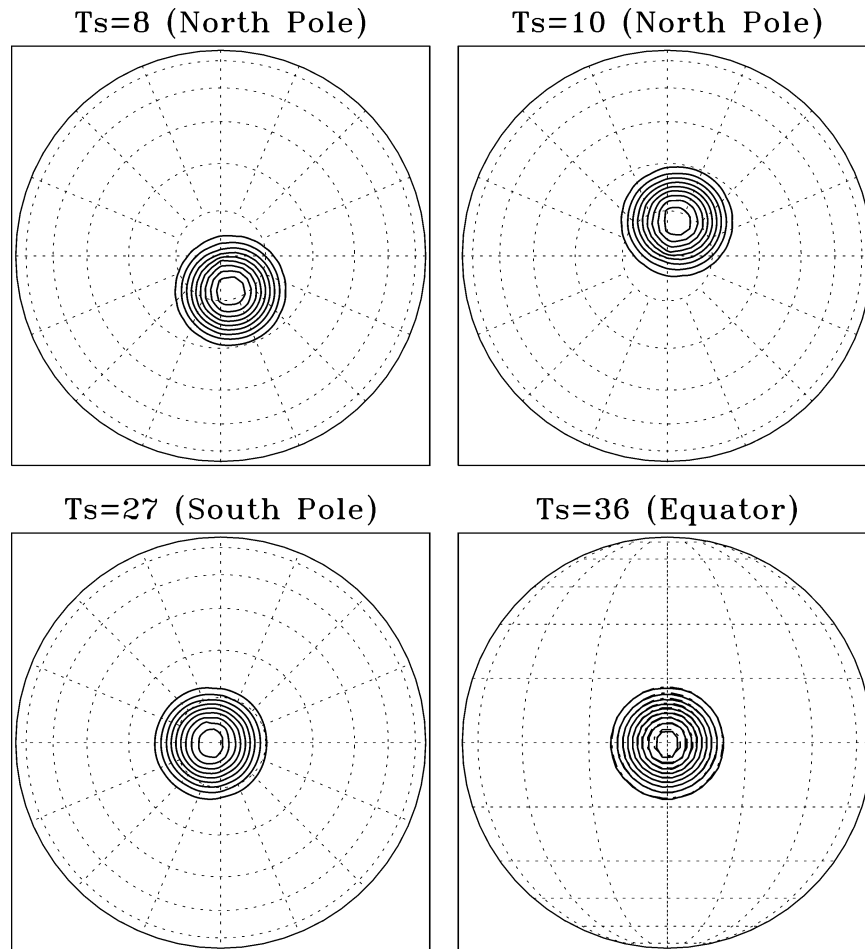
Ts=8 (North Pole)   Ts=10 (North Pole)

Ts=27 (South Pole)   Ts=36 (Equator)

FIG. 2. Orthographic projection for the offset ($\alpha = \pi/2 - 0.05$) solid-body rotation of a cosine bell approaching the North Pole at time step 8 (top left), crossing over the North Pole at time step 10 (top right), over the South Pole at time step 27 (bottom left), and over the equator at time step 36 (bottom right, initial position). The polar meridional Courant number is $C_\theta \approx 3.6$. The CCS combined with the CISL scheme is used for the numerical integration, and the exact solutions are shown as dashed contours.

gular belt (NSS02), implying that the CISL scheme is only needed when $C_\theta > 1$.

The cascade process begins by fitting the density distribution function (3) along the μ direction for every Eulerian cell. Because density distributions for both schemes are based on parabolic functions, the coefficients used for the CCS in the μ direction can be shared with those of the CISL scheme. The coefficients of the parabolas h_1, h_2 in (3) during the first phase of the cascade can be used for the polar CISL density distribution functions (4) such that $c = h_1$ and $d = h_2$. However, for the CISL scheme, the coefficients along the λ direction, a, b in (4) are computed independently (NM02).

3. Numerical tests

We consider two numerical experiments to test the extended CCS. In order to demonstrate the robustness of the scheme, the numerical experiments are set for large Courant numbers. However, for practical application the choice of time step (Courant number) is dictated by physical process, stability, accuracy, and efficiency considerations. The numerical tests are solid-body rotation of a cosine bell (Williamson et al. 1992) and nonsmooth deformational flow (Doswell 1984; NSS02) over the sphere. Exact trajectories are employed for both tests. For the solid-body rotation test, the orientation of the flow is chosen to be in the pole-to-pole direction. The value of the flow parameter α is set to $\pi/2$ or $\pi/2 - 0.05$ (Williamson et al. 1992). When $\alpha = \pi/2 - 0.05$, cross-polar advection can be simulated with slight off-centering of the cosine bell with respect to the poles, making the test more challenging. The computational domain consists of 128×64 grid cells spanning the surface of the sphere (see NSS02 for details). Angular velocity of the solid-body rotation ω is either $2\pi/36$ or $2\pi/72$ radians per time step so that 36
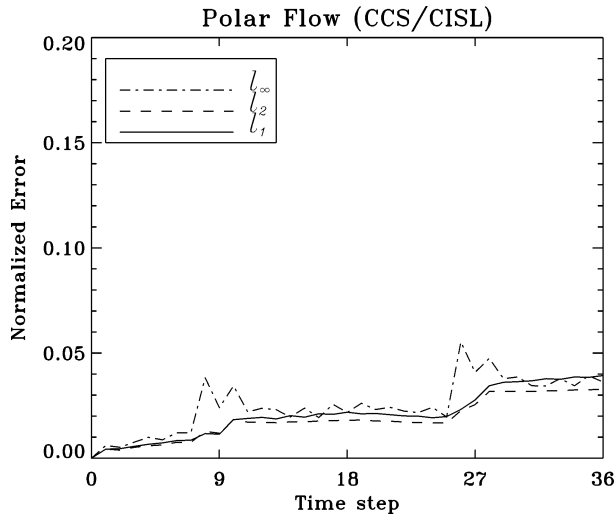
Polar Flow (CCS/CISL)

FIG. 3. Time series of l_1, l_2, and l_∞ errors for the solid-body rotation problem when the flow is along the pole-to-pole direction; 36 time steps are required for one revolution.

or 72 time steps are required for one complete revolution over the sphere. The corresponding polar meridional Courant number are $C_\theta \approx 3.6$ and $C_\theta \approx 1.78$, respectively.

The results for solid-body rotation of a cosine bell for the offset polar flow ($\alpha = \pi/2 - 0.05$) are shown in Fig. 2 (contour values vary from 0.1 to 0.9). The top panels show the cosine bell approaching (left) and leaving (right) the north pole at time steps 8 and 10, re-

spectively. The bottom panels show the cosine bell at time step 27 over the South Pole (left) and returning to the initial position at time step 36 (after one complete revolution). The initial solution is displayed in the bottom right panel using dashed contours. There is a slight distortion at the center of the bell when it crosses the poles. Note that no filter has been applied in either of the CCS/CISL schemes to suppress the noise generated at the poles. Figure 3 shows the time series of l_1, l_2, and l_∞ normalized errors for polar advection ($\alpha = \pi/2$). Oscillations in the plots are severe when the bell crosses the North and South Poles at time steps 9 and 27, respectively. The plots become relatively smooth when the bell moves away from poles, particularly for l_∞.

We have compared the normalized errors of the extended CCS with those of the CISL scheme in NM02. For this experiment, 72 times steps are used for the offset polar flow to complete one revolution. The l_1, l_2, and l_∞ errors for the extended CCS are, respectively, 0.038, 0.034, and 0.057, and the corresponding error values for CISL scheme are 0.041, 0.037, and 0.051. This indicates the extension process of CCS does not significantly impact the accuracy.

For the nonsmooth deformational flow, we chose the same test parameters in NSS02, except for the duration of the numerical integration. The initial and exact solutions after 2.5 time units are shown in Figs. 5a and 5b of NSS02 and are not given here. The number of time steps required for simulating the nonsmooth vortex
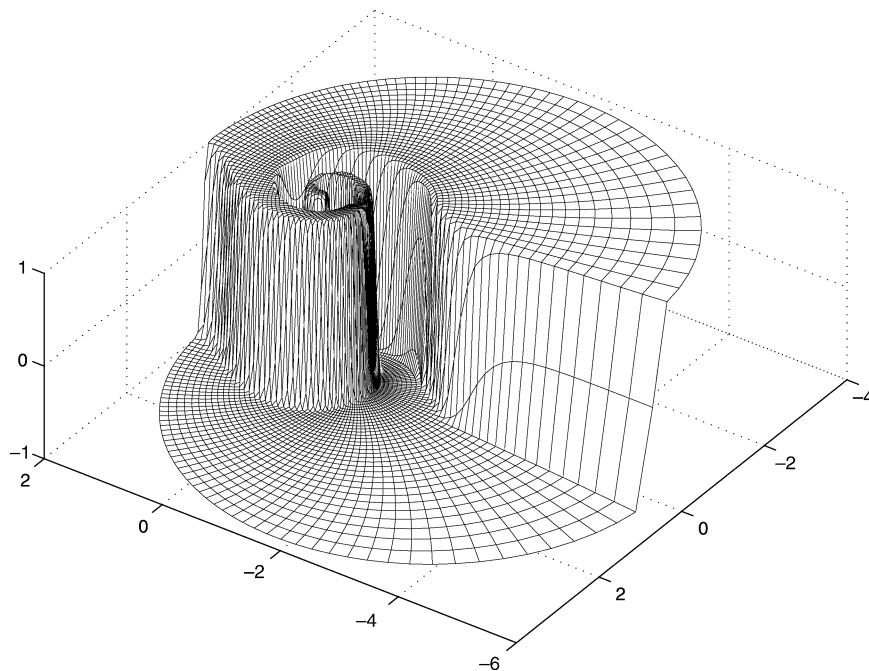

FIG. 4. Numerical solution of the nonsmooth deformational flow problem at $t = 2.5$ units (32 time steps), projected onto a plane tangent to the vortex center. The extended CCS with monotonic filter and with exact trajectories is used for the numerical integration.

for the present experiment is 32. This corresponds to maximum zonal and meridional Courant numbers $C_\lambda \approx$ 32 and $C_\theta \approx 1.6$, respectively. A monotonic version of the extended CCS was used for the integration. Figure 4 shows the numerical solution as projected onto a plane tangent to the vortex center. The numerical solution displayed in Fig. 4 is similar to Fig. 6 of NSS02. It shows that the extended CCS is capable of accurately handling even quasi-continuous solutions.

4. Summary and conclusions

The conservative cascade scheme (CCS) developed by Nair et al. (2002) combines mass-conservative finite-volume advection with a backward trajectory semi-Lagrangian method in a computationally efficient cascade interpolation framework. However, in conventional spherical geometry, the CCS is applicable only when the polar meridional Courant number is $C_\theta \leq 1$. In order to apply the CCS without this restriction on the sphere, polar regions where the CCS fails are isolated. A 2D remapping scheme, CISL (Nair and Machenhauer 2002), is applied within the isolated polar region when $C_\theta > 1$. The interface between CCS and CISL is designed to be the polar singular region, where certain Lagrangian cells are either deformed or not well defined. Total mass in the polar singular region is computed and redistributed to the individual Lagrangian cells by a simple scheme developed by Nair and Machenhauer (2002). This scheme is a local approximation but is constrained to be conservative. The resulting extended CCS scheme was tested for solid-body rotation and deformational flow using large Courant numbers. The test results show that the extended CCS is accurate for cross-polar advection. Monotonic options of CCS/CISL may be used for producing monotonic solutions.

The execution time of the CCS on the sphere is almost half that of the CISL scheme (Nair et al. 2002). Because the CISL scheme is only applied over a small region on the sphere, the overall computational efficiency of the extended CCS is not seriously affected. For realistic 3D applications such as a climate model (Williamson et al. 1998), the extended CCS may be suitable because it is conservative, efficient, and free from the polar meridional Courant number limitations.

References

Colella, P., and P. R. Woodward, 1984: The piecewise parabolic method (PPM) for gas-dynamical simulations. *J. Comput. Phys.,* **54,** 174–201.

Doswell, C. A., III, 1984: A kinematic analysis of frontogenesis associated with a nondivergent vortex. *J. Atmos. Sci.,* **41,** 1242–1248.

Lin, S.-J., and R. B. Rood, 1996: Multi-dimensional flux-form semi-Lagrangian transport schemes. *Mon. Wea. Rev.,* **124,** 2046–2070.

Machenhauer, B., and M. Olk, 1996: On the development of a semi-Lagrangian cell integrated shallow water model on the sphere. *Proc. ECMWF Workshop on Semi-Lagrangian Methods,* Reading, United Kingdom, ECMWF, 231–228. [Available from ECMWF, Shinfield Park, Reading, Brekshire RG2 9AX, United Kingdom.]

Nair, R. D., and B. Machenhauer, 2002: The mass conservative cell-integrated semi-Lagrangian advection scheme on the sphere. *Mon. Wea. Rev.,* **130,** 649–667.

——, J. Côté, and A. Staniforth, 1999: Cascade interpolation for semi-Lagrangian advection over the sphere. *Quart. J. Roy. Meteor. Soc.,* **125,** 1445–1468.

——, J. S. Scroggs, and F. H. M. Semazzi, 2002: Efficient conservative global transport schemes for climate and atmospheric chemistry models. *Mon. Wea. Rev.,* **130,** 2059–2073.

——, ——, and ——, 2003: A forward trajectory semi-Lagrangian scheme over the sphere. *J. Comput. Phys.,* **190,** 275–294.

Purser, R. J., and L. M. Leslie, 1991: An efficient interpolation procedure for high-order three-dimensional semi-Lagrangian models. *Mon. Wea. Rev.,* **119,** 2492–2498.

Rasch, P. J., 1998: Recent developments in transport schemes at NCAR, MPI workshop on conservative transport schemes. Max Planck Institute for Meteorology MPI Tech. Rep. 265, 65–75. [Available from Max Planck Institute for Meteorology, Bundesstrasse-55, D-20146, Hamburg, Germany.]

Williamson, D. L., J. B. Drake, J. Hack, R. Jacob, and P. N. Swartz-trauber, 1992: A standard test set for numerical approximations to the shallow water equations in spherical geometry. *J. Comput. Phys.,* **102,** 211–224.

——, J. G. Olson, and B. A. Boville, 1998: A comparison of semi-Lagrangian and Eulerian tropical climate simulations. *Mon. Wea. Rev.,* **126,** 1001–1011.

Zerroukat, M., N. Wood, and A. Staniforth, 2002: SLICE: A semi-Lagrangian inherently conservative and efficient scheme for transport problems. *Quart. J. Roy. Meteor. Soc.,* **128,** 2801–2820.